CEDAR 2014
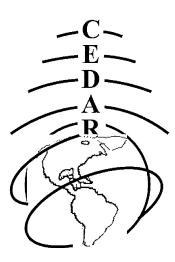
Cascade Ballroom, Haggett Hall
University of Washington

Seattle, Washington

MLT Poster Session
Wednesday June 25, 2014

"CEDAR Grand Challenges"

Table of Contents

Coupling of the Upper Atmos with Lower Alts

Instr or Techniques for Middle Atmosphere Obs

Long Term Variations of the Mesosphere and Lower Thermosphere

Meteor Science other than wind observations

Mesosphere and Lower Thermosphere Gravity Waves

Mesosphere and Lower Thermosphere Lidar Studies

Mesosphere or Lower Thermosphere General Studies

Mesosphere and Lower Thermosphere Other Tidal, Planetary Waves, or Sudden Stratosphere Warnings

Sprites

CEDAR Workshop – MLT Poster Session Abstracts
Day 2 – Wednesday, June 25, 2014

Coupling of the Upper Atmos with Lower Alts

COUP-01   **Daily variation of diurnal thermal tides from CHAMP and GOCE accelerometer measurements -** by Gasperini, Federico

Status of First Author: Student IN poster competition, PhD

Authors: Jeffrey M Forbes; Kathrin Haeusler; Maura Hagan; Sean Bruinsma; Eelco Doornbos

Abstract: Daily migrating and non-migrating diurnal tides in exospheric temperature derived from simultaneous accelerometer measurements on CHAMP (near 300 km) and GOCE (near 260 km) are studied for the intervals November-December 2009 and March-April 2010. Neutral densities are converted to exospheric temperatures using the NRLMSISe00 empirical model and by iterating on a convenient parameter (e.g. F10.7 solar flux). This methodology is validated using NCAR TIME-GCM simulations for this period as a mock data set, and results are compared to an approach where differences between ascending and descending orbital measurements are used to estimate diurnal tides for CHAMP and GOCE separately. The tidal components analyzed are the westward-propagating components with zonal wave numbers s=1 and s=2 (DW1 and DW2) and the eastward-propagating components with s=-2 and s=-3 (DE2 and DE3). Spectral analyses are used to reveal potential planetary wave modulations of the daily tidal amplitudes.

COUP-02   **Investigating ocean-ionospheric coupling -** by Grawe, Matthew A.

Status of First Author: Student NOT in poster competition, Undergraduate

Authors: Matthew A. Grawe, Pierdavide Coisson, Thomas W. Gehrels, Daniel J. Fisher, Jonathan J. Makela

Abstract: Within the past decade, several tsunami events have occurred in the Pacific Ocean. Analysis of upper atmospheric parameters through the utilization of GPS-derived total electron content (TEC) and airglow imaging systems during these tsunami events suggests a potential link to ocean wave amplitude. Of special importance are the 2011 Tōhoku event and another event occurring in 2012 on the Haida Gwaii archipelago in Canada for which clear signatures of ocean-ionosphere coupling are evident. These two cases provide limiting examples that can be used to study how the orientation of the wave fronts with respect to the magnetic field affect the efficiency of coupling between the neutral fluid and ionosphere.

COUP-03   **Ionospheric vertical plasma drift perturbations due to the quasi-2 day wave -** by Gu, Sheng-Yang

Status of First Author: Student IN poster competition, PhD

Authors: Han-Li Liu, Tao Li, Xiankang Dou

Abstract: The Thermosphere-Ionosphere-Mesosphere-Electrodynamics General Circulation Model is utilized to study the vertical ExB drift perturbations due to the westward quasi-2 day wave (Q2DW) with zonal wavenumber 2 and 3 (W2 and W3). The simulations show that both wind components contribute directly and significantly to the vertical drift, which is not merely confined to low latitudes. The vertical drifts induced by W2 are much larger than W3 due to the stronger wind oscillations at E wind dynamo region. The vertical drifts induced by the total wind perturbations of W2 maximize at the equator and are much larger than by any individual component, while the vertical drifts from W3 maximize at middle latitudes and are comparable with from the individual component. This is because the vertical drift perturbations induced by the zonal and meridional winds of W2 are nearly inphase, whereas the ion drift perturbations are out of phase for W3.

COUP-04   **Tidal-Induced net transport effects on the oxygen distribution in the thermosphere -** by Jones, Jr., McArthur

Status of First Author: Student IN poster competition, PhD

Authors: Jeffrey M. Forbes, Maura E. Hagan

Abstract: We report on a series of numerical experiments performed with the National Center for Atmospheric Research (NCAR) Thermosphere-Ionosphere-Mesosphere-Electrodynamics General Circulation Model (TIME-GCM), designed to evaluate a new mechanism by which the dissipation of vertically-propagating tides act to change the atomic oxygen (O) distribution in the thermosphere. Jones et al. [2014] were the first to propose that the tides induced a net transport of constituents themselves, in addition to the transport provided by the mean circulation that is driven by dissipation of tides [Yamazaki and Richmond, 2013]. Through diagnosis of the continuity equation for the atomic oxygen number density, [O], our results show that the net meridional and vertical transport of O induced by the tides appreciably contributes to [O] changes in the lower thermosphere. Combined with recombination these transport mechanisms drive a net reduction in [O] of order 25% that is transmitted to higher altitudes by molecular diffusion. The migrating diurnal tide appears to be the main driver of the [O] variations during September, with the migrating semidiurnal tide playing a greater role in December.

COUP-05   **Coupling of the northern polar vortex to mesospheric temperatures during Sudden Stratospheric Warming -** by Kim, Jeong Han

Status of First Author: Non-student, PhD

Authors: Jeong-Han Kim, Geonhwa Jee, Young-In Won, Baek-Min Kim, Seong-Joong Kim

Abstract: We have been operated an IR spectrometer in Kiruna, Sweden (67.90°N, 21.10°E) since 2001 to measure the OH nightglow emissions in near infrared and analyzed daily temperatures during 2004 through 2011 as well as the daily data from Aura/MLS instrument and MERRA reanalysis, in order to study the relationship between the variation of polar vortex in stratosphere and mesospheric temperature change at northern high latitude. In this study, we investigated the height profiles of correlation coefficients between daily polar cap index (PCI) anomaly at 10 hPa, which represent the variability of polar vortex, and area-mean mesospheric temperature anomalies over 60°N during northern winters for the period described above. While most of previous studies have used the zonal mean temperature for the comparison of stratospheric and mesospheric temperatures, our result using the daily area-mean temperature and polar cap index at 10 hPa showed not only the mesospheric cooling in lower mesosphere but also the warming in upper mesosphere during SSW events, which is consistent with the result of Siskind et al. (2005) using TIMED/SABER temperature data. We also present the comparison of our results with that from WACCM simulation.

COUP-06 **The dependence of ionospheric densities on small electrostatic fields in the mesosphere and lower ionosphere -** by Salem, Mohammad A.

Status of First Author: Student NOT in poster competition, PhD

Authors: Mohammad Salem, Ningyu Liu, and Hamid K. Rassoul

Abstract: Transient luminous events (TLEs) manifest the direct coupling between the lower and the upper atmospheres. They are caused by strong electric fields established temporarily in the upper atmosphere by lightning activities at tropospheric altitudes. Many studies have been devoted to investigating the effects of TLEs in the upper atmosphere. It has also been demonstrated that thunderstorms can modify ionospheric densities on a longer time scale, during which TLEs may or may not occur [e.g., Cheng and Cummer, Geophys. Res. Lett., 32, L08804, 2004; Shao et al., Nat. Geosci., doi: 10.1038/NGEO1668, 2012]. In the work presented here, we study how even a small electrostatic field that may exist in the upper atmosphere during a thunderstorm can affect local ionospheric densities.

Our study is conducted by using a relatively simplified ion chemistry model described by Liu [J. Geophys. Res., 117, A03308, 2012]. The model is based on the one developed by Lehtinen and Inan [Geophys. Res. Lett., 34, L08804, 2007], which is in turn an improved version of the GPI model discussed in Glukhov et al. [J. Geophys. Res., 97, 16971, 1992]. According to this model, charged particles can be grouped into five species: electrons, light negative ions, cluster negative ions, light positive ions, and cluster positive ions. In this study, we assume steady state solutions of the electron and ion densities are reached when a small electrostatic field is present in the upper atmosphere.

In our chemistry model, the three-body reaction is the only one whose rate constant depends on the electric field. We first compare the rate constants of this reaction from different sources, and formulate the most reliable values in the electric field range of interest to our study. Finally, we examine any appreciable changes in ionospheric densities as a result of the small electric field in the upper atmosphere.

COUP-07 **Comparison of TIME-GCM/MERRA simulated tides with LEO satellite observations -** by Haeusler, Kathrin

Status of First Author: Non-student

Authors: K. Haeusler, M. E. Hagan, X. Zhang, J. M. Forbes, E. Doornbos, S. Bruinsma, and G. Lu

Abstract: We report on National Center for Atmospheric Research (NCAR) thermosphere-ionosphere-mesosphere-electrodynamics general circulation model (TIME-GCM) simulations for the year 2009. We apply the recently developed lower boundary condition based on three-hourly MERRA (Modern-Era Retrospective Analysis for Research and Application) reanalysis data to account for tropospheric waves and tides propagating upward into the model domain. The solar and geomagnetic forcing is based on prevailing geophysical conditions. We quantify the global-scale variability of the neutral temperature in the upper thermosphere on multiple time scales and focus on tidal and planetary wave signatures. We extract TIME-GCM densities along the Gravity Field and Steady-State Ocean Circulation Explorer (GOCE) satellite orbit to enable direct model-measurement comparisons in order to assess TIME-GCM performance. We also compare and contrast modeled exospheric tidal temperatures with determinations from combined Challenging Minisatellite Payload (CHAMP) and Gravity Recovery And Climate Experiment (GRACE) satellite observations to further elucidate the variability of TIME-GCM and to quantify the uncertainties associated with the satellite exospheric temperature determination technique.

COUP-08 **Simulations of the effects of vertical transport on the Thermosphere and ionosphere using two coupled models -** by Drob, Douglas Patrick

Status of First Author: Non-student

Authors: Douglas P. Drob, D.E. Siskind, K.F. Dymond, and J.P. McCormack

Abstract: We have explored the sensitivity of the thermosphere and ionosphere to dynamical forcing from altitudes near the mesopause (∼ 95 km) as recently described by Siskind et al., (2014). We show results from five simulations, all for the year 2009, with the NCAR/Thermosphere Ionosphere Electrodynamics General Circulation Model (TIEGCM). Two simulations were driven with the NCAR Global Scale Wind Model (GSWM) and three used output from the Advanced Level Physics High Altitude (ALPHA) version of the Navy's Operational Global Atmospheric Prediction System (NOGAPS). Use of NOGAPS-ALPHA allows for realistic meteorological variability from the lower atmosphere to propagate up into the TIEGCM, including a rich spectrum of non-migrating tides. We find that the additional vertical transport from these tides causes a significant reduction in the calculated peak electron density of the ionospheric F2 layer (NmF2). The mechanism for this effect is the enhanced downward transport of atomic oxygen to the base of the thermosphere. In turn, this yields a greater relative abundance of N2 and hence, enhanced recombination of ions and electrons. To get improved agreement with observed electron densities, we must reduce (Kzz) by a factor of 5. However, even with lower Kzz, our calculation still underestimates the NmF2 compared with radio occultation observations by the Constellation Observing System for Meteorology, Ionosphere and Climate (COSMIC) satellite system. This underestimate of NmF2 may be linked to an overestimate of the non-migrating tides in the coupled TIEGCM-NOGAPS calculations or to uncertainties in the bottom boundary for atomic Oxygen in the TIEGCM. We explore the second hypothesis by actively constraining the bottom boundary of the TIEGCM to observed atomic oxygen values from the NASA TIMED/SABER instrument. This work sponsored by the Office of Naval Research.

COUP-9   Effects of the Migrating Terdiurnal Tide in the Ionosphere and Thermosphere - by Cook, Matthew W.

Status of First Author: Student IN poster competition, Undergraduate

Authors: Matthew W. Cook [1], Jian Du [1], Jia Yue [2] and Lutz Haberzetti [1]
[1] Department of Physics and Astronomy, University of Louisville, Louisville, KY, USA
[2] Department of Atmospheric and Planetary Science, Hampton University, Hampton, VA, USA

Abstract: The upward propagating terdiurnal tide has recently been suggested to modulate the composition and dynamics of the thermosphere, thus changing the electron density in the ionosphere. The current NCAR/HAO Thermosphere Ionosphere Electrodynamics General Circulation Model (TIEGCM) only includes migrating and nonmigrating diurnal and semidiurnal tides in its lower boundary at ~97 km. For this analysis, we introduce the migrating terdiurnal tide parameters (temperature, horizontal winds, and geopotential height) from a climatological run of the extended Canadian Middle Atmosphere Model (eCMAM) into the lower boundary of the TIEGCM. The effects of the migrating terdiurnal tide in the thermosphere and ionosphere are examined by comparing the result to a model run of the TIEGCM that does not consider the terdiurnal tide. Some of the interesting thermosphere and ionosphere anomalies (such as the equatorial mass density anomaly and the midnight temperature anomaly) are particularly investigated to examine to what extent their correct representations in the model depend on whether or not the terdiurnal tide was considered.

COUP-10   Study of relationships between the ionospheric and thermospheric tidal signatures using theoretical models - by Lin, Charles

Status of First Author: Non-student

Authors: Charles Lin, Yu-Tsung Chen, Loren C. Chang, Po-Cheng Chen, Jia-Ting Lin, Joseph Huba and Chia-Hung Chen

Abstract: Variations of the ionospheric electron density structures related to the tidal forcing propagating upward from the lower atmosphere have been studied intensively recently. The longitudinal variations of ionospheric electron density are related to the thermospheric nonmigrating tidal signatures produced in-situ or propagating upward from below. During a stratospheric sudden warming, thermospheric migrating tidal signatures are modified and lead to the phase shift of ionospheric electron density structures at low latitudes. With the increasing number of global ionospheric observations, it is desirable to relate the thermospheric tidal signatures to corresponding tidal signatures of ionospheric electron density, since the neutral thermospheric temperature and wind observations are rather limited. In this paper we perform theoretical simulations to study the interconnections between tidal modes in thermospheric neutral parameters and ionospheric plasma. The migrating and nonmigrating tides of thermospehric winds at solar maximum and minimum periods are output from NCAR GSWM/TIEGCM runs. These thermospheric tides are further incorporated to NRL SAMI-3 to investigate the responses of corresponding tidal modes in ionospheric electron density and their physical meanings.

Instruments or Techniques for Middle Atmosphere Observations

ITMA-01   **Triboelectric current measurements from a multi-surface Langmuir probe in the mesosphere -** by Barjatya, Aroh

Status of First Author: Non-student

Authors: Martin Friedrich, Boris Strelnikov

Abstract: We present results from a recent mesospheric rocket flight from Andoya Rocket Range that carried a novel multi-surface Langmuir probe. Three fixed bias Langmuir probes with different surfaces: Stainless Steel, Nickel and Platinum were exposed to the mesospheric plasma environment. In addition to collecting thermal electrons, each surface is expected to interact differently with the neutral constituents of the mesosphere: neutral metal atoms, mesospheric smoke particles, ice particles, etc. We attempt to back out these particle densities from the Langmuir probe current measurements.

ITMA-02   **Multistatic Specular Meteor Radar -** by Rainville, Nicholas

Status of First Author: Student IN poster competition, PhD

Authors: Nicholas Rainville

Abstract: Winds in the upper atmosphere are responsible for distributing energy throughout Earth's atmospheric system; knowledge of these winds is necessary in order to accurately model both the behavior of the upper atmosphere as well as Earth's climate as a whole. Historically, these winds have been measured with Traditional Specular Meteor Radar (TSMR.) TSMR is a VHF radar system with a collocated transmitter and receiver, which senses reflections off the ionized trails of ablating meteors. These trails shift with the motion of the neutral wind in the mesosphere and by recording the motion of these trails the overall wind field in that region can be observed. However since the reflections are specular, the meteor trail must be nearly tangent to a sphere centered at the receiver antenna location. This limiting geometry also restricts wind velocity measurements to the direction radial to that sphere; many trails must be combined to view large-scale wind structures. The number of trails observed as well as the angular diversity of the wind velocity measurements can be greatly improved by adding additional phase coherent radar receivers to the radar system, to form a Multistatic Specular Meteor Radar (MSMR.)

An MSMR can provide both increased spatial and temporal resolution of the wind measurements, since instead of requiring the meteor trail to align with a single sphere any trail tangent to an ellipse described by

a transmitter receiver pair is in view. Adding additional receivers then increases the number of visible meteors as well as the number of visible trail angles. If the multiple receivers are spread over 100s of km, they also improve the observation radius to 10s of thousands of kms, compared to roughly 600 km for a single receiver. However, synchronizing the phase of geographically distributed MSMR receivers presents additional challenges over a TSMR. Development of a software defined radar platform combined with a GPS synchronized oscillator is under way to meet this additional requirement. Developing a flexible, low cost, and open hardware platform also enables the deployment of a large network of MSMR transmitters and receivers, which in turn can provide improved upper-atmospheric wind measurements as well as observations for meteor physics. An initial MSMR deployment will be tested the summer of 2014 by PhD candidate Cody Vaudrin under an NSF EASPSI award, and a subsequent deployment has been proposed to the NSF CNIC program for collaboration with the Leibniz Institute of Atmospheric Physics.

ITMA-03 Spectral Width Calculations from Mesospheric Turbulent Layers Detected from JRO and SOUSY - by Robinson, Rebecca Anne

Status of First Author: Student IN poster competition, Masters

Authors: Gerald Lehmacher, Jennifer Smith

Abstract: MST radars around the world have been used to collect signatures of neutral and plasma turbulent layers in the middle-to-upper atmosphere as functions of time and altitude. We present an analysis of mesospheric echo data collected at the Jicamarca Radio Observatory in April of 2011. From previous work, it is known that estimates of horizontal and vertical winds in the mesosphere can be determined by the spectral width of the Doppler velocity spectra. A similar analysis was performed on this data set from April of 2011. We present calculations of spectral widths within turbulent layers of the mesosphere and comment on any physical and temporal trends. Additionally, we suggest possible sources of contamination due to broadening of the radar beam, as well as provide a comparison between the different beams and two radar arrays (JRO and SOUSY) used in this experiment.

ITMA-04 Mesospheric winds obtained from simultaneous 30MHz and 50MHz All-sky Specular Meteor Radars at Jicamarca - by Scipion, Danny Eddy

Status of First Author: Non-student, PhD

Authors: D. Scipion, G. Sugar, and M. Milla

Abstract: A new 30 MHz Jicamarca All-sky Specular METeor radar (JASMET) was installed at the Jicamarca Radio Observatory (JRO) in August 2013 primarily for testing and validation before its final deployment for routine operations at the Observatory in Huancayo, Perú. Validation of the wind estimates is obtained by comparing estimates with those taken from JRO's 50 MHz JASMET system. These systems detect meteors that satisfy the specular condition wherein the meteor's trajectory is perpendicular to the broadcasted signal. The detection of three or more specular meteors by the different receivers allows the estimation of mesospheric winds from 70 – 110 km altitude because the Doppler shift is independent of the meteoroid's velocity.

Three main campaigns were performed after the radar's installation. The first campaign was from 22-23 August 2013, the second one from 28 October – 2 November 2013, and the third one from 14-16 April 2014. Both systems operated simultaneously, and independent observations were obtained. The first observations show that the 30 MHz radar detected more meteors than the 50 MHz radar, most likely, because the 30 MHz radar has higher sensitivity to meteors with lower plasma densities. We will compare wind profiles obtained from both radars and compare both with profiles obtained from the daytime mesospheric echoes measured with the main Jicamarca IS radar measured during the Oct 2013 campaign.

**ITMA-05   QB50 - Multipoint, In-Situ, Measurements of the Lower Thermosphere via
                CubeSat Constellation -** by Stark, Johnathon

Status of First Author: Student IN poster competition, Masters

Authors: Johnathon P. Stark

Abstract: The QB50 project is an initiative born out of the Belgian von Karman Institute to place
approximately fifty double and triple CubeSats into low Earth orbit. The mission's overall objectives are to
demonstrate the feasibility of launching a network of fifty, university built, CubeSats as a primary payload;
conduct multipoint, in-situ measurements of the largely unexplored lower thermosphere; provide an
educational opportunity for the participating universities; and facilitate access to space. The CubeSats
themselves will each carry one of the primary flight instruments, an Ion/Neutral Mass Spectrometer
(INMS), a Flux φ Probe Experiment (FIPEX), or a multi-Needle Langmuir Probe (mNLP).

A consortium of four U.S. schools, the University of Michigan, the Universidad del Turabo, the University
of Colorado, and Stanford University in cooperation with Draper Labs and the National Science Foundation
are proposing to fly four CubeSats as part of the QB50 project. Named in honor of the space shuttle
Challenger, the CubeSat being built at the University of Colorado will fly an INMS instrument as its
primary payload. In order to support this payload, the student team at the University of Colorado is
designing a custom Attitude Determination and Control System (ADCS) to enable the CubeSat to point the
INMS sensor head to within 10° of the velocity vector and allow for attitude knowledge to within 2°.

**ITMA-06   Lower Atmosphere/Ionosphere Coupling Experiment CubeSat Mission
                (LAICE) -** by Westerhoff, John

Status of First Author: Student NOT in poster competition, PhD

Authors: Dr. Gary Swenson, Dr. Greg Earle, Dr. Alex Ghosh

Abstract: LAICE is a groundbreaking experiment in LEO focused on understanding how waves generated
by weather systems in the lower atmosphere propagate and deliver energy and momentum into the
mesosphere, lower thermosphere, and ionosphere (MLTI). These waves are a vitally important but under-
explored facet of atmospheric physics. They strongly influence the dynamics of the media through which
they travel by modifying the structure of the atmosphere at altitudes well above their source regions, and
they may seed the development of plasma instabilities that scintillate and disrupt radio propagation. Our
experiment will be the first global satellite investigation to focus entirely on these waves, and to attempt to
connect their causes and effects in three widely different altitude ranges.
In-situ instrumentation will measure the perturbations the waves produce in both neutral and ion densities
at F-region heights, while on-board photometers will simultaneously measure the wavelengths and
amplitudes of the wave fields in the upper mesosphere. Subsequent modeling coupled with meteorological
data will reveal the connections between tropospheric storms and the MLTI system using state-of-the-art
ray tracing techniques that include the effects of wave dissipation. Our mission will combine the expertise
of scientists at four different institutions to substantially add to our knowledge of a critical coupling process
between disparate atmospheric regions, while providing hands-on learning experiences in space systems
engineering to over 60 students at two universities.

ITMA-07   Wind and Temperature Observations with ERWIN-II –
                by Kristoffersen, Samuel

Status of First Author: Student IN poster competition, PhD

Authors: Samuel Kristoffersen, William Ward

Abstract: The ERWIN-II (improved E-Region Wind Interferometer) is a Michelson interferometer which measures mesospheric winds via Doppler shifts in emissions from several airglow layers. The observed airglow layers are the atomic oxygen green line (557.7 nm at ~97 km), O_2 (866 nm at ~94 km) and OH (843 nm at ~87 km). The ERWIN-II is located at Eureka, Nu (80 N, 86 W) at the Polar Environment Atmospheric Research Laboratory (PEARL). Through use of a quad mirror in the optical train, ERWIN-II is able to make simultaneous high precision (~1 m/s for green line and OH, and ~4 m/s for O_2) wind measurements in the four cardinal directions (north, east, south, and west) and zenith, at a very high observational cadence (~3 minute cycle through all three emissions). This combination of high precision and observational cadence allows the observation of vertical winds, high frequency phenomena (e.g. gravity waves), as well as tides and planetary waves. Additionally, atmospheric temperatures can be determined from the observed airglow line visibilities. Observations of gravity waves in both the wind and irradiance measurements, the correlations between these measurements, and preliminary atmospheric temperature measurements will be presented.

Long Term Variations of the Mesosphere and Lower Thermosphere

LTVM-01   The Influence of CO2 Concentration and F10.7 Variations on Mesospheric Airglow Emissions - by DiMenichi, Chris

Status of First Author: Student IN poster competition, Undergraduate

Authors: Chris DiMenichi and Tai-Yin Huang

Abstract: CO2 concentration level measured in Mauna Loa has shown to increase steadily over the past 60 years, and based on a theoretical study by Roble and Dickinson [1989] it should cause a decrease in the number density of the major gas species and cooling in the Mesosphere/Lower Thermosphere (MLT) region. Previous theoretical study by Huang [2014] investigates the effects of CO2 concentration variation on various airglow emissions in the MLT region. There have been quite a few studies on variations of airglow emissions caused by the 11-year variations in F10.7, although no definitive correlation has been established. In this present study, we will examine the combined effect of CO2 concentration level increase and F10.7 variations on mesospheric airglow emissions like OH(8,3) Meinel band, O2(0,1) atmospheric band, and the O(1S) greenline emission. The OH Chemistry Dynamics model and the Multiple-airglow Chemistry Dynamics model are used for the investigation. The CO2 concentration levels and F10.7 values from 1980-1991 will be used in this study to investigate the impact of the solar cycle combined with the increased CO2 concentration level within that time period.

LTVM-02   Temperature response to the 11-yr solar cycle in the eCMAM30 simulation and SABER observation - by Gan, Quan

Status of First Author: Student IN poster competition, PhD

Authors: Quan Gan; Jian Du; Shaodong Zhang

Abstract: In the present work, the zonal mean temperature from 31-yr (1979-2010) extended Canadian Middle Atmosphere Model (eCMAM) simulation and 12-yr SABER/TIMED (2002-2013) observation are analyzed to study the temperature response to the 11-yr solar cycle from the lower stratosphere to the lower thermosphere. Multiple linear regression method is performed on the de-seasoned data at each latitude and altitude for both data sets. By considering various factors, which may potentially induce the interannual variability of zonal mean temperature, the regression analysis includes the QBO, ENSO and 11-yr solar cycle terms for SABER data and one more term associated with volcanic eruption for eCMAM data.The annual mean and seasonal variability of zonal mean temperature response to solar cycle will be discussed

and compared between eCMAM and SABER. The combined solar cycle and QBO effects will also be discussed in the paper.

LTVM-03   **Nonmigrating tidal impact on carbon dioxide 15 µm infrared cooling of the lower thermosphere over one solar cycle -** by Nischal, Nirmal

Status of First Author: Student IN poster competition, PhD

Authors: Nirmal Nischal, Jens Oberheide, M. G. Mlynczak, and L. A. Hunt

Abstract: This paper explores the impact of diurnal and semidiurnal solar atmospheric tides that begin near the surface as heat is released by evaporation and condensation on the energy budget of the lower thermosphere: the carbon dioxide (CO_2) infrared cooling of the thermosphere at 15 µm. Cooling rates of CO_2 observed by SABER/TIMED from 2002-2013 are analyzed on three important nonmigrating tides, the DE3, DE2, and SE2. Relative amplitudes are on the order of 25% with respect to the monthly mean emissions. Seasonal and solar cycle variations are discussed and complemented to nitric oxide 5.3 µm emissions. Our results further support the idea that tropospheric tides due to large-scale weather systems are not only important for the dynamics and electrodynamics of the ionosphere-thermosphere system but also for the energy budget of Earth's upper atmosphere.

LTVM-04   **A multi-year analysis of Rayleigh lidar measurements from the Poker Flat Research Range in Chatanika, Alaska -** by Triplett, Colin Charles

Status of First Author: Student IN poster competition, PhD

Authors: Robin Wind, Kohei Mizutani, and Richard L. Collins

Abstract: A review of a multi-year analysis of Rayleigh lidar measurements taken from Lidar Research Laboratory-Poker Flat Research Range (LRL-PFRR) in Chatanika, Alaska (65 N, 147 W) is presented. In this analysis Rayleigh lidar observations from August-May 1997-2014 is used to create a set of reference data for the arctic middle atmosphere. This set will include, but not be limited to, nightly temperature profiles, density fluctuations, and gravity wave potential energy. In this analysis we have developed consistent data retrieval techniques for data taken in varying atmospheric conditions and signal levels. This analysis will extent to scope of a recent IPY study to include higher altitude investigations, temperature fluctuations, and gravity wave propagation. Besides being a reference data set, this analysis will be used in the understanding of gravity waves around mesospheric inversion layers (MILs) in tandem with the upcoming MTeX rocket campaign.

Meteor Science other than wind observations

METR-01   The mesospheric potassium layer: updated results from the OSIRIS satellite dataset - by Dawkins, Erin

Status of First Author: Student IN poster competition, PhD

Authors: E. Dawkins, J.M.C. Plane, M.P. Chipperfield, W.Feng., J. Gumbel, J. Hedin, J. Haffner and J. Friedman

Abstract: Changes in the mesosphere are an important signal of climate change and there is increasing evidence that accurate simulations of changes to the Earth's climate require models with a well resolved

and accurate stratosphere and mesosphere. Following the ablation of meteoroids, the resulting metal species which are injected into the mesosphere/lower thermosphere region (80-110 km) offer a unique way of observing this region and of testing the accuracy of climate models in this domain.

A sodium retrieval algorithm first developed by Gumbel et al. (2007, GRL) has been extended, and modified to retrieve potassium densities using data from the OSIRIS spectrometer on-board the Odin satellite. Here we present an overview of the new potassium retrieval scheme, along with the first ever climatology of the global potassium layer from space for 2004-2011. These layers have been validated using lidar data and successfully capture the unusual semi-annual seasonal behaviour of potassium, which is starkly different to the other metals. Unlike sodium and iron which both display early wintertime density maxima, potassium also displays a summertime maximum which points to some unique and surprising features in the chemistry and the way it interacts with other atmospheric species. A detailed potassium chemistry scheme, developed by a team at Leeds (UK) (modules for Na, Fe, Ca and Mg already added), has now been included in a version of the NCAR Whole Atmosphere Community Climate Model (WACCM), which also includes a meteor input function model first developed by Janches et al. (2006, JGR). The annual, latitudinal and long-term variation of these modelled potassium layers are compared with the retrieved datasets to evaluate model chemistry and dynamics. This new model of K chemistry correctly simulates, for the first time, the unusual seasonal variation of the K layer.

METR-02 Assessing the threat that meteoroid generated plasmas pose to spacecraft - by Fletcher, Alexander

Status of First Author: Student IN poster competition, PhD

Authors: Alexander Fletcher, Sigrid Close

Abstract: Spacecraft are routinely bombarded with interplanetary dust particles, called meteoroids, and defunct objects of human origin, called space debris. Meteoroids have impact speeds up to 72 km/s and space debris have impact speeds less than 11 km/s in low Earth orbit. Most hypervelocity impactors possess enough energy to ionize and vaporize themselves as well as a significant portion of the spacecraft material upon impact, forming a plasma that rapidly expands into the surrounding vacuum. The associated electrical effects and potential for damage to satellite electronics through these processes remains largely unknown.

We present an update on computational multi-physics simulations of particle impacts on spacecraft using continuum mechanics and particle-in-cell. These simulations incorporate elasticity and plasticity of the solid target, phase change and plasma formation, strongly coupled plasma physics due to the high density and low temperature of the plasma, a fully kinetic description of the plasma, and free space electromagnetic radiation.

By simulating a series of hypervelocity impacts, we determine basic properties (e.g. temperature, expansion speed, charge state) of the plasma plume for impact speeds of 10-72 km/s. We find for impact speeds of 30-72 km/s, the temperature approaches an asymptote of 2.5 eV; this relatively low temperature agrees with our recent ground-based experiments. We also find that the plasma plume is weakly ionized for impact speeds less than 14 km/s and fully ionized for impact speeds greater than 20 km/s. This is the same threshold for the measured electromagnetic pulses. We find that in idealized cases, we find the plasma can produce fields that could be threatening to spacecraft electronics if they are nearby the point of impact. Understanding key parameters of impact plasma plumes, as well as any RF emission mechanisms, will aid in designing more robust and reliable spacecraft that are well protected in the space environment.

METR-03 Phase De-aliasing of Point Targets Observed with Jicamarca 50 MHz Array Radar Using Multi-Baseline Receiving Modules - by Gao, Boyi

Status of First Author: Student IN poster competition, PhD

Authors: Boyi Gao and John D. Mathews

Abstract: The Jicamarca 50 MHz Array Radar (Lima, Peru) has been employed to study meteors using its interferometric mode for decades. Although the main radar array has the capability of transmitting high power (approximately 2 megawatts) and detecting point targets with high angular precision, the phase ambiguity introduced by the nature of interferometry makes it hard for researchers to determine the actual altitudes of the observed meteors. The largest ambiguity circle available for single-baseline interferometry using adjacent module-receivers is $\pm4.78°$. By employing the multi-baseline module-receiving configuration introduced in this study, which is adding a portable Yagi-array receiver outside the main radar array, the effective ambiguity circle is enlarged to $\pm30°$ in the direction which the extra module is added. If two portable module receivers could be added to two orthogonal interferometric baselines respectively, it would increase the "unambiguous" solid angular coverage of the sky by 40 times without the need to update any of the existing hardware. Also, when taking into consideration the Jicamarca narrow beam, whose half-power beam width is only $\sim2°$, this new radar configuration is sufficient to exclude the commonly raised "side lobe contamination" objection to the existence of high-altitude radar meteors (HARMs). This new implemented radar configuration adds a new feature to the array system without compromising any of the other desirable features, such as high sensitivity, high directivity, and high angular precision. In addition, the phase de-aliasing method described in this study makes the seemingly complicated process as simple as finding matches in a lookup table, which reduces the computational time dramatically.

METR-04   **Meteor detection algorithm in optical and radar measurements -**
             by Limonta, Lorenzo

Status of First Author: Student NOT in poster competition, PhD

Authors: Lorenzo Limonta, Robert Marshall, and Sigrid Close

Abstract: A key problem for accurately modelling the behaviour of the atmosphere is its neutral density in the upper layers (80-300 Km). In this poster we present an automated technique to detect meteoroid in radar and optical measurements. Subsequently the obtained measurement are used to analyse composition of the meteors as well as to estimate property of thesurrounding density

METR-05   **Initial Results from Simultaneous Optical and Radar Meteor Observations
             at Poker Flat Research Range -** by Sugar, Glenn

Status of First Author: Student IN poster competition, Masters

Authors: Glenn Sugar, Bob Marshall, and Sigrid Close

Abstract: We present results from a joint optical and radar experiment conducted at the Poker Flat Research Range over three nights in April 2014. Meteors were observed using the Poker Flat Incoherent Scatter Radar (PFISR), as well as two high speed sensitive cameras, an Andor iXon Classic and an Andor iXon Ultra. The iXon Classic was equipped with a long pass filter (>475nm) in order to estimate meteoroid composition. We investigate meteors that were observed by all three instruments and compare the independent measurements of meteoroid mass. We also present new estimates for the meteor ionization coefficient and luminous efficiency.

METR-06   Correlation Between Non-Specular Radar Meteor Trails and Corresponding Head Echo Data - by Tarano, Ana Maria

Status of First Author: Student IN poster competition, Masters

Authors: Ana M. Tarano and Sigrid Close

Abstract: Meteoroids entering the Earth's atmosphere are detected by high-power, large aperture (HPLA) radars as they ablate in the E-region of the ionosphere between 140 and 70 km altitude. The radar returns can be classified as head echo, the plasma traveling with the meteoroid, and trail, the expanding plasma column left in the meteoroid's wake. A non-specular trail, a distinct type of trail, is thought to be reflections from field-aligned irregularities (FAI) forming after the onset of plasma turbulence. These particulars trails are detected when the radar beam is pointed quasi-perpendicular to the magnetic field.

A detection algorithm was conceived to efficiently examine data collected at the Advanced Research Project Agency (ARPA) Long-range Tracking and Identification Radar (ALTAIR). The ALTAIR data comprised dual frequency, dual polarized, and high range resolution in-phase (I) and quadrature (Q) returns with azimuth and elevation data obtained from the monopulse system.

Synthesizing understanding of range and time dependence of meteor events with image processing techniques, the algorithm localizes the head echo and its corresponding non-specular trail. The detection algorithm additionally permitted the characterization of head echo and non-specular trail features, such as duration, altitude of occurrence, and signal-to-noise ratio (SNR) depending on frequency and polarization. Hence, the located head echo and trail pairs were then examined to define the time and range delays between the detection of the head plasma and that of the trail. These statistics demonstrated that faster meteoroids lead to shorter time delays and longer lags in range. Moreover, detections starting at higher altitudes showed longer postponements in time and range between the reflections of the head echo and the non-specular trail.

METR-07   Freedom from Matched Filter Constraints: Sparse Decomposition of Radar Signals for Delay-Frequency Sidelobe Removal - by Volz, Ryan

Status of First Author: Student IN poster competition, PhD

Authors: Sigrid Close

Abstract: A sparsity-based radar waveform inversion technique is formulated and found to significantly improve observations of ionospheric plasma, resulting in cleaner data that limits self-interference of range-spread targets and enables differentiation in crowded and variable environments. Taking direction from the theory of compressed sensing, sparsity or compressibility of the radar target scene is employed as prior knowledge to remove processing artifacts caused by the standard matched filter approach. Because these delay-frequency sidelobe artifacts are removed, this technique enables new experiment modes using waveforms that are unsuitable for matched filtering. The real-world flexibility and effectiveness of the inversion technique is demonstrated on meteor observations made simultaneously with a variety of standard waveforms using the Jicamarca high-power large-aperture radar. Though the approach has been applied to ionospheric radar, it is generally applicable and especially relevant for radar target scenes with multiple or distributed scatterers.

METR-08   To establish the automatic observation system for the fantastic luminous phenomena and the Taiwan Elegant Meteor and TLE Network - by Yang, I-Ching

Status of First Author: Non-student

Authors: I-Ching Yang, Hsin-Chang Chi, Shinsuke Abe, Chi-Long Lin, Jing-Yuan Ko, Chun-Chieh Tsao, Bing-Xun Wu

Abstract: Using high-sensitivity charge-coupled device (CCD) and video record software, UFOCapture, at Taitung and Kaohsiung we establish the automatic observation system for the fantastic luminous phenomena in the night sky. By way of artificial selection to eliminate the non-meteor's video, the trajectory, luminosity and position of meteor can be analyzed from the meteor's video by using UFOAnalyzer. Then, to integrate these data of tow observation stations, the velocity and height of meteoroid might be calculation precisely by the method of triangulation, and it is possible to obtain the orbit related to the Sun and origination of meteoroid. In 2012, to associate with several automatic observation systems around Taiwan, we organized the Taiwan Elegant Meteor and TLE Network (be abbreviated to TWEET).

METR-09 Implications of Aspect Sensitivity and Frequency Dependence on Nonspecular Meteor Trail Turbulence - by Yee, Jonathan

Status of First Author: Student IN poster competition, PhD

Authors: Sigrid Close

Abstract: As a meteoroid ablates in Earth's atmosphere, it produces a plasma referred to as a head, which is the plasma that surrounds the meteoroid, and a trail, which is the quasi-stationary plasma behind the meteoroid. High Power, Large Aperture radars have become an important tool in characterizing both heads and trails. Of particular interest is a subset of trails known as nonspecular trails that are thought to be reflections from field aligned irregularities that form due to the onset of turbulence in the trail. In this paper, we present the results of an investigation into nonspecular trail and head echo dependence on detection frequency and the angle between radar boresite and the background magnetic field. These data, collected at the Advanced Research Project Agency Long-range Tracking and Identification Radar, include dual frequency and polarization, and high range resolution in-phase and quadrature returns with azimuth and elevation angles. We present nonspecular trail analysis results that confirm clear aspect sensitivity in both detection frequencies. In addition, we show that not only are the number of detections diminished, but also the time duration of detected nonspecular trails falls as the angle between radar boresite and background magnetic field changes from 90º. We then demonstrate that there is a detection frequency dependence of nonspecular trails and their detection properties. We finish by suggesting a theory that the turbulence at the core of nonspecular trail detections could be, in fact, anisotropic with length scales that may produce a scattering difference resulting in the aspect sensitivity and frequency dependence in trail detections.

METR-10 Radar Holography via joint sparsity model - by Zhu, Qian

Status of First Author: Student IN poster competition, PhD

Authors: Qian Zhu and John D. Mathews

Abstract: Given a relatively few available measurements, compressed sensing has been demonstrated as an effective signal processing method. By implementing the joint sparsity compressed sensing model, this paper provides new results regarding to the application of compressed sensing to radar holography. A straightforward method is to model the holography problem by the single measurement vector model. While simple, the single sparsity model ignores valuable correlation structure in the signal that can be explored to improve the recovery performance. Therefore, by taking into account the correlation property of signal, the proposed joint sparsity model for radar holography can not only significantly reduce the computational complexity, but also produce high resolution and detection accuracy.

METR-11 **The Altitude Distribution of Iron Monoxide in the Mesosphere** by Evans, Wayne F.J.

Status of First Author: Non-student

Authors: W.F.J. Evans, NWRA and York University, R.L. Gattinger and E.J. Llewellyn , University of Saskatchewan

Abstract:
- Cosmic dust enters the mesosphere and ablates into a hot gas which later condenses into meteoritic smoke, leaving behind some atomic iron in the gas phase.
- This atomic iron has been measured extensively with iron lidars at several sites . The atomic iron reacts with ozone to form iron oxide, FeO. The FeO reacts with atomic oxygen to recycle the atomic iron, Fe. This balance between production and loss leads to a small stable concentration of molecular FeO. Although there are side cycle reactions of FeO with other gases, they are not important above 80 km .
- The reaction of Fe with ozone leads to a chemiluminescent airglow emission, previously discovered by the authors from their OSIRIS spectrograph on the ODIN satellite.
- The intensity of this airglow emission from $FeO(^5D)$ is proportional to the product of the atomic iron concentration and the ozone concentration. Since the rate for the reaction of FeO with atomic oxygen is in equilibrium with rate of reaction of Fe with ozone, the airglow intensity can be used to derive the FeO density if the atomic oxygen concentrations are available. The atomic oxygen can be derived from other airglow emissions, in particular the A band of O_2 , simultaneously observed by the OSIRIS instrument.
- An observed Fe profile was also derived and compared with LIDAR Fe measured profiles.
- The optical efficiency of the reaction of Fe with ozone was estimated to be about 16%.
- Plan to expand the coverage of Fe by melding OSIRIS profiles with LIDAR profiles.

Mesosphere and Lower Thermosphere Gravity Waves

MLTG-01 **Comparison of parameterized gravity forcing in WACCM and eCMAM and their effect on the Diurnal Tide -** by Agner, Ryan Matthew

Status of First Author: Student IN poster competition, PhD

Authors: Ryan M. Agner, and Alan Z. Liu

Abstract: In most Global Circulation Model's (GCM's), gravity waves (GW) are too small to be directly simulated due to the current computational limits so a parameterization scheme has to be employed to include their effects. It has been shown that the thermal tides in the mesopause region in GCM's are sensitive to the GW parameterization scheme used. For example, GCMs which use the Lindzen type parameterization such as the Whole Atmosphere Community Climate Model (WACCM) tend to suppress the diurnal tidal amplitude while those that use the Hines Doppler Spread Parameterization such as the Extended Canadian Middle Atmosphere Model (eCMAM) tend to increase the diurnal tidal amplitude. The current work investigates the differences in gravity wave forcing between the WACCM and the eCMAM on a spacial and seasonal basis. The effect that the diurnal components of the two parameterization schemes have on the amplitude and phase of the diurnal tide is then studied to gain insight into the difference of gravity wave-tide interactions in these models based on different GW parameterization schemes.

MLTG-02   Mountain waves observed with an All Sky Imager at the Andes Lidar Observatory - by Aguilar Guerrero, Jaime

Status of First Author: Student IN poster competition, Masters

Authors: Alan Z. Liu, Fabio Vargas, Gary R. Swenson, Anthony Dominic Mangognia

Abstract: All sky airglow imagers are an important tool for assessing the occurrence of gravity waves events in the mesopause region. They can probe more than half a million square kilometers of the airglow layer where small and large scale structures are observable. This work examines mountain waves observed with the all sky imager at the Andes Lidar Observatory located in Cerro Pachón, Chile, from years 2009-2014 (current). For characterizing Mountain Gravity Waves, several interactive tools have been developed for exploring parameters such as duration, frequency and amplitude; these tools include user interfaces that are embedded in nightly keograms that allow for dynamic smoothing, flat-fielding, unwarping (geographic projection) and intensity threshold setting for each night. A large database has been generated with the processed data that contains images, videos and keograms for every night of available data. A compiled data set like this one allows for further statistical analysis such as seasonal variations and frequency of events. This information is essential in exploring and determining the sources and mechanics of Mountain Waves that occur at this particular location. Preliminary results of identified mountain waves and their parameters are compiled using these tools.

MLTG-03   Intermittency of Gravity Wave Momentum Flux in the Mesopause Region Observed with All Sky Imager in Maui and Cerro Pachón - by Cao, Bing

Status of First Author: Student IN poster competition, PhD

Authors: Bing Cao, Alan Z. Liu, Zhenhua Li, Chester S. Garder

Abstract: The intermittency of gravity wave momentum flux in the mesopause region is investigated for the first time using data from all-sky OH airglow imager at Maui (20º48'N,156º20'W), Hawaii and Cerro Pachón (30º14'S,70º44'W), Chile. The probability density functions (pdfs) of momentum flux show two distinct regions of distribution. For momentum flux less than 12-15 m2/s2, the pdfs follows a log-normal distribution; at the tail for larger momentum flux, they deviate from the log-normal distribution and follow a power-law distribution. The fitted parameters from these two different types of pdfs can be used to quantify the intermittency of the gravity waves. Overall the intermittency at Cerro Pachón is larger than that at Maui. This is likely associated with the larger intermittency of orographically generated gravity waves over the Andes, as compared to convectively generated gravity waves over the Pacific Ocean. The intermittency of the gravity waves in both locations shows some seasonal variation.

MLTG-04   UV albedo perturbations produced by gravity waves as seen from space - by Carstens, Justin Neal

Status of First Author: Non-student, PhD

Authors: Justin N. Carstens, Scott M. Bailey, M. Joan Alexander, Cora E. Randall

Abstract: Nadir images of Rayleigh scattered UV sunlight (265 nm) from the Cloud Imaging and Particle Size (CIPS) instrument on the Aeronomy of Ice in the Mesosphere (AIM) satellite contain many periodic structures. These structures are believed to be the result of Gravity Waves (GW). In this work, we investigate the theoretical impact of GWs on the albedo imagery. We show that GWs are indeed capable of producing the observed structures and present the range of GWs which are capable of producing measureable albedo perturbations CIPS imagery. The sensitivity to GW perturbations peaks at an altitude of ~50 km with a FWHM of ~15 km. For most viewing geometries, CIPS is sensitive to GW with vertical

wavelengths longer than ~15 km with relative GW amplitudes on the order of 1% in temperature or density. The field of view limits sensitivity to horizontal wavelengths less than a few hundred km, and resolution limits sensitivity to horizontal wavelengths greater than ~20 km. This translates to a sensitivity to waves with an intrinsic period shorter than ~2 hrs.

Existing satellite GW studies in this altitude region use limb scanners or microwave nadir imagers, which are sensitive to much longer horizontal wavelengths. This tends to limit the sensitivity to longer period waves. Therefore, the addition of CIPS imagery to the existing coverage of GW measurements is complimentary - significantly expanding the spectral coverage of GWs near the stratopause. GWs are critically important to middle atmosphere dynamics, and their representation in global climate models is not well constrained by observations.

MLTG-05   **The 11-year Solar Cycle Signature on Gravity Waves -**
by Cullens, Chihoko Yamashita

Status of First Author: Non-student

Authors: Scott England

Abstract: The impacts of the 11-year solar cycle on gravity waves are investigated using WACCM simulations and SABER observations. In this study, we conducted 50 years of free running WACCM simulations to study responses of gravity waves to the 11-year solar cycle. For these 50-year simulations, we output all gravity wave components, and it allows us to separate gravity wave responses by their sources and phase speeds. Our results show that the largest 11-year solar cycle signals on gravity wave drag exist at high-latitudes in winter from the stratosphere to the lower thermosphere. It is likely caused by the responses of planetary wave activities to the 11-year solar cycle. In addition, relationship between solar cycle, stratospheric sudden warming (SSW), and quasi-biannual oscillation (QBO) will be discussed.

MLTG-06   **Simulating Thermospheric Optical Observations in the Presence of a Gravity Wave -** by Fisher, Daniel J.

Status of First Author: Student IN poster competition, PhD

Authors: Daniel J. Fisher, Jonathan J. Makela, Sharon L. Vadas, Timothy M. Duly, Pierdavide Coisson

Abstract: Gravity waves play an important role in energy transfer in the atmosphere, depositing momentum in both the mesosphere and thermosphere. While current modeling results show that gravity waves should occur frequently with a great amplitude in the thermosphere, very few ground-based optical instruments have captured this phenomena. A series of cases have been run to simulate what a red line all-sky imager and Fabry-Perot interferometer would measure for a gravity wave propagating through the thermosphere. We present results from both a circular and linear gravity wave perturbation. We will present how the relationship between the viewing geometry and the gravity wave orientation affects the measurements.

MLTG-07   **Thermospheric Gravity Wave Observations over Alaska Using the Poker Flat Incoherent Scatter Radar -** by Negale, Michael R.

Status of First Author: Student IN poster competition, PhD

Authors: M. R. Negale, K. Nielsen, M. J. Taylor, M. J. Nicolls

Abstract: It is now well known that atmospheric gravity waves play important roles in the mesosphere lower thermosphere (MLT) region (~80-110 km) through momentum deposition. Observational and modeling studies in the past decade have revealed the importance of these waves in the higher thermospheric region (~110 – 400 km) as they contribute significantly to changes in both winds and temperatures. Although case studies have revealed their presence in the thermosphere, the distributions and variability of thermospheric gravity wave parameters are currently unknown. Recently, a collaborative observational effort utilizing Rayleigh lidar, an all-sky airglow imager, and the Poker Flat Incoherent Scatter Radar (PFISR) has been performed over interior Alaska to study a broad spectrum of gravity waves throughout the troposphere, mesosphere, and thermosphere. This presentation details the process of obtaining wave parameters from the Poker Flat Incoherent Scatter Radar (PFISR) (based on a method developed by Nicolls and Heinselman, 2007) and presents preliminary wave characteristic distributions for the winter season of 2010 – 2011. These distributions are compared to results obtained with the mesospheric airglow imager co-located at Poker Flat Research Range.

**MLTG-08   The Effects of Gravity Waves on Airglow Temperatures in the MLT Region
- by George, Richard**

Status of First Author: Student NOT in poster competition, Undergraduate

Authors: Tai-Yin Huang

Abstract: We investigate gravity wave effects on airglow temperature fluctuations and secular variations in the Mesosphere/Lower Thermosphere (MLT) region. We also investigate the phase differences for airglow intensity and temperature. These investigations are conducted using a 2-D OH Chemistry Dynamics (OHCD) and a Multiple Airglow Chemistry Dynamics (MACD) model. Both models include a spectral full wave model that provides gravity wave forcing and an airglow chemistry model that simulates time evolution of airglow species. The OHCD model includes the OH(8,3) nightglow chemistry and the MACD model includes the O(1S) Greenline and O2(0,1) atmospheric band nightglow chemistry. Temperatures of these airglow emissions are the focus of our investigations. The differences between different temperatures (rotational temperature, Doppler temperature, and intensity-weighted temperature) will also be discussed.

**MLTG-09   Vertical Na and heat flux by gravity waves over the Andes Lidar
Observatory - by Guo, Yafang**

Status of First Author: Student IN poster competition, PhD

Authors: Yafang Guo, Alan Z. Liu, Chester S. Gardner, Gary R. Swenson, Anthony Dominic Mangognia, Fabio Vargas

Abstract: By using the high resolution Na Doppler lidar measurements, located at Andes Lidar Observatory, Cerro Pechón, Chile (30.0S, 71.0W), the vertical fluxes of heat and constituent induced by dissipating gravity waves are derived from vertical wind, temperature and sodium density profiles between 85 and 100 km. All the vertical fluxes are corrected for the bias due to photon count noises. The heat flux bias has a magnitude ranging from -0.6 K m/s to -0.13 K m/s from the edge to middle of the altitude range. The heat flux profile shows downward transport in the mesopause region with two maxima of 0.68K m/s and 0.55K m/s at 90.5 km and 95.5 km, respectively. This flux is smaller in magnitude compared with the previous results obtained from Maui (20.7N, 156.3W) and Starfire Optical Range (35.0N, 106.5W) but has similar vertical structure. Comparison between winter and summer profiles shows slight difference in structures and values. The vertical Na flux also has two downward maxima with a magnitude of 89.9 cm-3ms-1 and 96.4 cm-3ms-1 almost at the same altitudes as the heat flux. The dynamical Na flux associated with dissipating gravity waves estimated from the heat flux is consistent with the measured Na flux below 94 km.

MLTG-10   Calculation of Gravity Wave Altitude Limits - by Hall, Stephen

Status of First Author: Student IN poster competition, PhD

Authors: Gary R. Swenson

Abstract: Vertical propagation of atmospheric gravity waves (AGW's) is constrained in the middle atmosphere by diffusion processes. These AGW's are a key component of energy and constituent transfer in this region, but propagation is limited to those altitudes for which the wavelength and period are less than the time and distance scales of the diffusion of those constituents. Using the 1976 Standard Atmosphere Model, it is possible to calculate these diffusion scales and thereby determine the propagation altitude limit of these AGW's based on their period and wavelength. This theoretical study should provide a method for better understanding energy transfer in this region of the atmosphere.

MLTG-11   Numerical simulations of small-scale gravity wave propagation through horizontally and vertically varying background winds -
by Heale, Christopher

Status of First Author: Student IN poster competition, PhD

Authors: J.B. Snively

Abstract: While small scale gravity wave propagation through vertically-sheared winds has been well studied [e.g. Bretherton., 1966; Hartman., 1975; Dunkerton and Fritts., 1984], relatively less attention has been paid to propagation through horizontally-varying winds. These include studies investigating wave propagation in horizontally sheared flows [e.g. Badulin et al., 1985; Badulin and Shrira., 1993; Huang et al., 2008] and in winds that vary along the direction of the flow [e.g. Basovich and Tsimring, 1984]. Naturally, horizontally varying flows arise in the atmosphere due to the presence of waves, tides, and jets of different horizontal scales. Linear theory predicts that the horizontal wavelength should increase or decrease depending on whether the background wind is increasing or decreasing in magnitude along the wave's horizontal propagation direction. This causes the phase angle to become more horizontal or vertical respectively, refracting the wave packet. Basovich and Tsimring, [1984] note an effect known as a 'blocking point' which occurs when the wind opposes the wave propagation direction and has sufficient magnitude to cause the waves horizontal group velocity to go to zero.

We investigate linear propagation of small-scale gravity waves through both horizontally and vertically varying background winds, and simulate the effects of medium scale wave wind fields on the propagation of small-scale gravity waves. We find that simulation results show good agreement with linear theory for smoothly varying flows. We also see the predicted effect of a horizontal 'blocking level' in which the horizontal group velocity of the gravity wave goes to zero and horizontal propagation ceases, while the horizontal wavelength decreases. The wind velocity at which this occurs is predicted well by the theory of Basovich and Tsimring, [1984]. We note that waves of small scales and short period are quite susceptible to this effect such that even small magnitude winds can modify the horizontal propagation of the wave packet.

MLTG-12   Vertical Evolution of Gravity Wave Potential Energy and Spectra from 30 to 110 km at McMurdo (77.8°S, 166.7°E), Antarctica - by Lu, Xian

Status of First Author: Non-student, PhD

Authors: Xian Lu, Xinzhao Chu, Zhibin Yu, Weichun Fong, Cao Chen

Abstract: We provide the first characterization of gravity wave vertical wavenumber spectra and potential energy from 30 to 110 km in the three winter seasons (2011–2013) at McMurdo, Antarctica. The potential

21

energy density per unit mass (Epm) grows exponentially with a mean scale height of ~12 km in the Rayleigh region (30–70 km), where waves are partially dissipated or saturated. In the MLT region, however, the vertical variation of Epm is not uniform. An unusually rapid increase of Epm is observed from 86 to 94 km with a scale height close to freely propagating waves (~6km), suggestive of either small dissipations or additional wave sources. Above 94 km, Epm increases slowly implying that gravity waves could dissipate severely. The mesopause is around 98 km, above which atmosphere is more stable and below it less stable. This is not consistent with more dissipation above the mesopause, implying that shear instability may contribute for significant wave dissipation above 94 km. The slopes of the vertical wavenumber spectra are about -2.2 and -2.7 in the MLT and Rayleigh regions, which do not match the theoretical prediction of -3 by linear saturation theory. In addition, the power spectral density in the MLT region is about 5-10 times larger than the Rayleigh counterpart, which can not be explained by the vertical variation of N2 according to linear saturation theory. It implies that nonlinear process is important for wave spectrum and should be considered in the theory.

MLTG-13 **A coordinated study of high-frequency gravity waves using lidars and temperature mapper -** by Lu, Xian

Status of First Author: Non-student, PhD

Presented by: Jian Zhao, PhD Student

Authors: Xian Lu, Jian Zhao, Xinzhao Chu, Dominique Pautet, Mike Taylor, Titus Yuan

Abstract: A remarkable signature of gravity wave with a period of ~1h is shown in the vertical wind on Nov 27, 2013 from the STAR sodium (Na) lidar measurement in Boulder, CO. Similar wave signatures are also observed in its temperature and Na density variations. The vertical wavelength of this 1-h wave is about 40 km. By combining the USU lidar and temperature mapper from which gravity wave oscillations with a period of ~1h are also noticeable, we study the possibility of an identical wave source for the similar wave signatures observed at two different locations (about 500 km apart). We study both the horizontal and vertical structure of the wave and how it evolves temporally, horizontally and vertically. This coordinated study is able to provide a 3-D information of the gravity wave, which has been rarely reported before. The possible wave source is also suggested.

MLTG-14 **Gravity Wave Characterization and Ray-tracing over South Pole -** by Mehta, Dhvanit

Status of First Author: Student IN poster competition, PhD

Authors: Dhvanit Mehta, Andrew Gerrard, Yusuke Ebihara, Allan Weatherwax

Abstract: We present gravity wave observations from mesopause 557.7-nm OI all-sky data taken by a multi-wavelength all-sky imager located at South Pole, Antarctica. A number of gravity wave events from July 26, 2010 are observed, and their horizontal wave parameters measured. These are used alongside model winds to determine the full intrinsic parameters of the waves, which are fed into the FOREGRATS ray-tracing model to investigate possible wave sources.

MLTG-15 **Multi-Year Analysis of Short-Period Gravity Waves Over Alaska Under Various Stratospheric Weather Conditions -** by Nielsen, Kim

Status of First Author: Non-student

Authors: K. Nielsen, M. Negale, K. E. Johnson, A. Chandran, D.-P. Pautet, and M. J. Taylor

Abstract: We present a four-year analysis of short period gravity waves measured by an airglow imager situated in Poker Flat, Alaska (65 N, 147 W). The imager is the cornerstone of the mesospheric airglow imaging and dynamics (MAID) project. This project is a collaborative effort between Utah Valley University, University of Alaska, Fairbanks and Utah State University, and employs the NICT Rayleigh Lidar System together with support observations from the co-located MF Radar and the NSF sponsored Poker Flat ISR. The overarching goal of the project is to characterize the waves, their variability, and how stratospheric weather impacts the observed wave field. In the study presented here, four years of airglow imaging data have been analyzed to investigate wave characteristics, year to year and seasonal variability, and correlate the observed wave parameters to stratospheric weather phenomena including the Aleutian low, the polar vortex, and sudden stratospheric warming events.

MLTG-16   Initial Measurements of Mesospheric Gravity Waves over McMurdo, Antarctica - by Pugmire, Jonathan

Status of First Author: Student IN poster competition, PhD

Authors: Jonathan R Pugmire, Michael J. Taylor, P. Dominique Pautet, Yucheng Zhao

Abstract: The ANtarctic Gravity Wave Instrument Network (ANGWIN) is an NSF sponsored international program designed to develop and utilize a network of gravity wave observatories using existing and new instrumentation operated at several established research stations around the continent. The primary goal is to better understand and quantify large-scale gravity wave climatology and their effects on the upper atmosphere over Antarctica. ANGWIN currently comprises research measurements from five nations (U.S., U.K., Australia, Japan, and Brazil) at seven international stations. Utah State University's Atmospheric Imaging Lab operates all-sky infrared and CCD imagers and an Advanced Mesospheric Temperature Mapper (AMTM) imager at several research stations (Davis, Halley, Rothera, McMurdo, and South Pole). In this poster we present new measurements of short-period mesospheric gravity waves imaged from McMurdo Station (77°S, 166°E) on Ross Island. This camera has operated alongside the University of Colorado Fe Lidar during the past two winter seasons (March-September 2012, 2013). Image data were recorded every ~10 seconds enabling detailed measurements of individual gravity wave events in the infrared OH emission layer (~87 km). Here we present example wave data and novel measurements of the wave characteristics observed during these two winter seasons. The results are contrasted with other published and new ANGWIN wave measurements from around the continent.

MLTG-17   Gravity Wave Parameters over Eureka, Canada in 2008-2009 - by Vail, Christopher

Status of First Author: Student IN poster competition, Masters

Authors: William Ward

Abstract: The PEARL (Polar Environmental Artic Research Laboratory) All Sky Imager (PASI) has been in operation since 2007 at PEARL in Eureka, Nunavut, Canada. PASI is a CCD imaging system with six different spectral band narrow band filters. The filters installed in PASI are targeted at the following emissions: atomic sodium (at 589.3 nm), background (at 572.5nm), molecular nitrogen ion (at 427.8nm), atomic oxygen green line (at 557.7nm), atomic oxygen red line (at 630.0nm) and hydroxyl (at 720-910nm notched at 865nm due to the molecular oxygen). PASI takes an image on average every minute while cycling through the different filters with the hydroxyl filter interweaved between the other filters in the sequence.

This poster will present the automated analysis approach developed to detect gravity waves present in the images from PASI. The gravity wave parameters of interest are the background wind corrected phase

speed, intrinsic period, and propagation direction. In each image occurrences of these waves are defined in terms of horizontal spatial wavenumber, and phase. Temporal phase information is deduced from consecutive images which contain wave signatures with similar wavenumbers. Vertical wavelength is determined from consecutive images between the different filters using an approach similar to determining the temporal phase. Monthly variations of these quantities their correlation with each other during the 2008-2009 season will be presented.

MLTG-18 **Uncertainties on Gravity Wave Parameters Obtained from Nightglow Image Data -** by Vargas, Fabio

Status of First Author: Student NOT in poster competition

Authors: Fabio Vargas, Gary Swenson, Chet Gardner

Abstract: Gravity wave observable parameters are commonly obtained from spatial/temporal variations of the nightglow radiance recorded in all-sky images. With those parameters, key atmospheric quantities associated with wave energy dissipation, like energy/momentum flux and flux divergence, are estimated. While these wave field derivables are obtained routinely from the observables, the accuracy of such estimations has been poorly considered in gravity wave climatology studies. In this paper, we model the primary errors/biases in each assessed wave parameter and show that relatively small deviations in these observables quantities translate into enormous uncertainties in derivable quantities. In addition, we show that primary errors in the observables have different magnitudes and depend essentially on the technique used to monitor the nightglow.

Mesosphere and Lower Thermosphere Lidar Studies

MLTL-01 **Applications of Atomic Filters in Na Doppler Lidar -** by Barry, Ian Forest

Status of First Author: Student IN poster competition, Undergraduate

Authors: Ian F. Barry, Wentao Huang, John A. Smith, Weichun Fong, and Xinzhao Chu

Abstract: Designs of Na atomic filters are revisited in conjunction with recent improvements in the quality and resolution of Na Doppler lidars to achieve two scientific goals in atmospheric measurements of wind and temperature: downward extension of the range of these lidars into the lower atmosphere and useful daytime observation capability. In the past, Faraday filters have demonstrated increased SNR in daytime observations, allowing for the study of diurnal cycles and other atmospheric effects of solar radiation that would be impossible with only nighttime measurements. The application of double-edge filters in recent years to measurements in the lower atmosphere has hinted at the observation of gravity wave generation by convective processes and topography, in addition to the propagation of these waves upward to the more extensively studied Mesosphere and Lower Thermosphere (MLT) region. However, the results of daytime and lower-atmosphere observation attempts have to date included noise levels prohibiting useful scientific interpretation. To increase the SNR of these observations, the Faraday filter design has been optimized for adjustable magnetic field strength, and the unique double-edge filter design replaces the tuned FPI in previous designs with an atomic filter for absolute frequency calibration with simultaneous wind and temperature measurements. In both cases, improved temperature control for the Na atomic filters has led to greater stability and control over the respective filter functions. The improved optical efficiency of the Na lidar receiver system has extended the range of nighttime measurements up to 110 km with significantly higher SNR than many other lidar systems, and has resulted in measurements of Rayleigh scattering up to 60 km using the atomic double-edge filter, with greater temporal and spatial resolution than demonstrated ever before. Results have so far demonstrated higher accuracy of measurements in the lower atmosphere using the new double-edge filter design in conjunction with the STAR Na Doppler lidar system developed

by the Chu Research Group out of CIRES, which will also be used to obtain daytime observations with higher signal levels and less noise. The expansion of the scientific capabilities of the Na Doppler lidar system into the lower atmosphere and daytime observations will allow for more complete characterization of the atmosphere over a wider range of times and altitudes, prompting new areas of research related to gravity wave generation in the lower atmosphere, the effects of solar radiation during the day, and phenomena with longer periods requiring continuous observation spanning multiple days.

MLTL-02   Seasonal Variations of Relative Neutral Densities between 45 and 90 km Determined from USU Rayleigh Lidar Observations. - by Barton, David Lee

Status of First Author: Student IN poster competition, Undergraduate

Authors: David Barton; Vincent B. Wickwar; Leda Sox; Josh P. Herron

Abstract: A Rayleigh-scatter lidar operated at the Atmospheric Lidar Observatory (ALO; 41.7°N, 111.8°W), part of Center for Atmospheric and Space Sciences (CASS) on the campus of Utah State University (USU), collected extensive data between 1993 and 2004. From the Rayleigh lidar photon-count profiles, relative densities were determined throughout the mesosphere, from 45 to 90 km. Using these relative densities three climatologies were derived, each using a different density normalization at 45 km. The first normalized the relative densities to a constant; the second normalized them to the NRL-MSISe00 empirical model, which has a strong semiannual component; and the third normalized them to the CPC analyses model, which has a strong annual component. In each case the density profile for every night of a composite year was found by averaging the nighttime density profiles over a 31-day by 11-year window centered on that day. For each of these three cases, the average annual density profile was found by averaging all the days. Then the daily fractional differences were found relative to the annual density profile. Despite the different normalizations at 45 km, many common features were found in the seasonal behavior of the density profiles. One is a large seasonal variation maximizing in June at ~70 km. Another, above 80 km is a large shift in the maximum to earlier in the year. Another is a sharp density fall off at almost all altitudes in early October. While these density normalizations provide initial information about mesospheric behavior, the current lidar upgrade will enable us to add an absolute scale to the density profiles.

MLTL-03   Investigations on seasonal variations of Gravity waves forcing by Na lidar over Logan, Utah (41.7°N, 111.8°W) - by Cai, Xuguang

Status of First Author: Student IN poster competition, PhD

Authors: Xuguang Cai and Tao Yuan

Abstract: The nightly mean potential energy density E_p is used to estimate the gravity wave forcing over Logan, Utah, the west side of Rocky Mountain. We calculate E_p based on temperature data of continuous diurnal cycle observation days of Utah State University (USU) Na lidar from 2011 to 2013. Our method is tidal background removal, which used harmonic fit to separate background and perturbations and then calculating variance of nighttime temperature perturbations and mean of reconstructed background on each altitude to obtain nightly mean . Furthermore, our results were compared with those deduced from the other two traditional methods: one is the linear background subtraction using a 2-hour sliding window and the other is the high-pass filter with cut-off period 2-hour. It is found that the results of the other two methods are much smaller than those of the tidal background removal. The difference can be explained by the fact that there exist active GWs with period longer than 2 hour. Therefore, the linear background subtraction and the filter methods remove the components belonging to GWs and decrease the E_p. In addition, we present a statistic result of long period GWs from 2011 to 2013 including the vertical parameters.

MLTL-04   **Lidar observations of temperature climatology from 0 to 110 km and mechanism study of winter temperature tides of fast amplitude growth above 100 km at McMurdo (77.8S, 166.7E), Antarctica -** by Fong, Weichun

Status of First Author: Student IN poster competition, PhD

Authors: Weichun Fong, Xinzhao Chu, Xian Lu, Zhibin Yu, Brendan Roberts, Cao Chen, Wentao Huang, Zhangjun Wang, Tim Fuller-Rowell, Mihail Codrescu, Chester S. Gardner, Adrian J. McDonald

Abstract: Long-term and year round temperature measurements at high-southern latitudes are rare. Over 3500 hours of lidar data have been collected after the accomplishment of the installation of an Fe Boltzmann lidar system at McMurdo (77.8°S, 166.7°E), Antarctica since late 2010. We provide the preliminary temperature climatology based on lidar and radiosonde observations between 0 to 110 km from 2011 to 2013. We compare the seasonal variation of temperature climatology with other stations in Antarctica such as South Pole (90°S) and Rothera (67.5°S), such as annual and semiannual variations, mesopause temperature height, and stratopause temperature and height, and etc. We further investigate the cause of the differences with the help of other measurements, such as MF radar winds, or models, such as WAM and WACCM. Moreover, McMurdo is located at high magnetic latitude and is near the poleward edge of aurora oval that the geomagnetic activities might have more impacts at McMurdo than the other stations, for which is also a factor we must consider.

Also, the first characterization of diurnal and semidiurnal thermal tides in temperature from 30 to 110 km in the winter season (May through August) at McMurdo reveals that the diurnal and semidiurnal tidal amplitudes grow fast above 100 km and can reach at least 15 K near 110 km, which are exceeding that of the freely propagating tides originating from the lower atmosphere. Such fast growth exists for all Kp index cases and diurnal amplitude increases to 15-30 K at 110 km with larger Kp indices corresponding to larger tidal amplitudes and faster growth rates. In addition, the slopes of diurnal tidal phases become steeper above 100 km and the tidal phases barely change with altitude from 100 to 106 km. Combining with the significant amplitude increases, it implies that there may exist additional tidal sources near or above 100 km. Geomagnetic activity appears to be a dominant tidal source above 100 km but may not be the only one. Since the fast amplitude growth exists for quiet (Kp = 1) condition as well, it indicates that geomagnetic activity may cause an enhancement of temperature tides but other additional contributions are still needed, such as direct solar heating and chemical heating. In this paper, we utilize the coupled thermosphere ionosphere plasmasphere electrodynamics (CTIPe) model to investigate the possible sources/mechanisms that lead to the fast amplitude growth of tides as observed by lidar in the polar winter region.

MLTL-05   **Thermospheric sodium layers observed by lidars at five sites over China -** by Gao, Qi

Status of First Author: Student NOT in poster competition, PhD

Authors: Qi Gao,Xinzhao Chu, Xiankang Dou, Xianghui Xue

Abstract: We report the thermospheric sodium layers observed by different lidars located at Beijing (40.2N, 116.2E), Hefei (31.8N, 117.3E), Wuhan (30.5N, 114.4E), Lijiang (26.7N, 100.0E), and Haikou (19.5N, 109.1E). All of the observations are nocturnal. The occurrence rates of thermospheric sodium layers are 9.1% at Beijing (46 days in total 508 observation days), 10.4% at Hefei (36/346), 11.9% at Wuhan (11/92), 13.9% at Lijiang (5/36), and 11.5% at Haikou (24/208). The yearly and monthly distribution of the thermospheric sodium layers is analyzed, which shows they are observed all over the year, and a large proportion of them are likely to arise in spring and summer. Typically, the thermospheric sodium layers are usually observed in a series of days continuously and often at the same time in each day. We further analyze the wave characteristics in thermospheric sodium layers. Case studies of some considerable events are also held, for example, the 10 April 2012 event at Lijiang maybe shows an extent to nearly 165 km with an approximate downward phase of 1.40±0.09 m/s.

MLTL-06   **Daytime lidar soundings in the mesosphere: New results from IAP lidars at Kühlungsborn -** by Gerding, Michael

Status of First Author: Non-student

Authors: Michael Gerding, Maren Kopp, Josef Hoeffner, Franz-Josef Luebken

Abstract: Since 2010 regular temperature lidar soundings during day and night are performed at Kühlungsborn (Germany, 54°N, 12°E) by combination of RMR lidar and K resonance lidar. The soundings continue the existing time series of temperatures observed during the night since 2002. Overall, the profiles cover all ranges from the stratosphere up to the lower thermosphere, with a small gap around 80 km during the day. Daytime observations require spectral filtering of the received photons by a double Fabry-Perot etalon (~4 pm width) and spatial filtering by use of a narrow field of view (~0.06 mrad) in combination with an active beam stabilization. Daytime operation allows the detection of tidal waves in the mesosphere and lower thermosphere. We have calculated the diurnal variation of temperature profiles from monthly composites. We will present monthly mean amplitudes and phases for the diurnal, semidiurnal, and terdiurnal variation. In the stratopause region the diurnal component typically dominates with mean amplitudes of 1-2 K. The diurnal tide is then damped at ~60 km altitude where it has about the same amplitude as the semidiurnal and terdiurnal variation. Around the mesopause the diurnal tide grows again, having mean amplitudes of about 4 K, but a large variability. The RMR lidar is additionally capable for daytime observations of polar mesospheric clouds (PMC). PMC observations at mid-latitudes are of special importance, as they are generally rare compared to higher latitudes. Changes due to temperature trends might therefore be more pronounced. We will show recent results on the diurnal variation of PMC occurrence as well as the long-term variation based on our nighttime data set since 1997 by an older RMR lidar.

MLTL-07   **Direct measurements of vertical gravity-wave and eddy heat and Na fluxes in the mesosphere and lower thermosphere at Boulder (40°N, 105°W), Colorado -** by Huang, Wentao

Status of First Author: Non-student, PhD

Authors: Wentao Huang, Chester S. Gardner, Xinzhao Chu, John A. Smith, Weichun Fong, Ian F. Barry, Zhibin Yu

Abstract: The vertical transport by gravity waves and tides plays a fundamental role in establishing the thermal and constituent structures of the MLT region, but has not been thoroughly investigated by observations. In particular, direct measurements of vertical heat flux and metal constituent flux caused by dissipating but non-breaking waves are rare because of the critical demands on instruments, such as the simultaneous achievement of very small field-of-view, high spatial and temporal resolutions along with long-duration measurements. Such requirements are necessary to overcome various uncertainties to reveal the small quantities of the heat and constituent fluxes induced by dissipating waves. So far such direct observations have only been reported at Starfire Optical Range (SOR) in Albuquerque, New Mexico. Furthermore, estimate of eddy heat and constituent fluxes from the turbulent mixing generated by breaking waves is even more challenging due to the even smaller temporal and spatial scales of the eddy. Consequently, the associated coefficients of thermal (kH) and constituent (kzz) diffusion have not been well characterized and remain as large uncertainties in models. We attempt to address these issues with direct measurements of these fluxes using a Na Doppler at Boulder.
Since summer 2010, we have been operating a Na Doppler lidar at Boulder, Colorado. Over 200 nights of MLT temperature, vertical wind, and Na density data have been collected, which are suitable for direct flux measurements. From 2011 to October 2013, we made extensive Na lidar observations with greatly improved signal levels. These data covering each month of a full year will be used to characterize the

seasonal variations of heat and Na fluxes and to be compared with the pioneering observations at SOR. In November 2013, we upgraded the lidar with two new frequency shifters and a new data acquisition scheme, which are optimized for estimating eddy fluxes and reducing the measurement bias. Since then, we have been making observations to directly measure the eddy heat and Na fluxes for the first time. Such lidar observations at Boulder will certainly help advance the understanding on the vertical transport in the MLT region and provide crucial observational references to the models.

MLTL-08   First lidar observation of the mesospheric nickel layer - by Li, Jintai

Status of First Author: Student IN poster competition, PhD

Authors: Jintai Li, Cameron M. Martus, Kohei Mizutani, and Richard L. Collins

Abstract: Ground-based resonance lidar has been used to detect the mesospheric nickel (Ni) layer. We present the detailed signal-noise-ratio(SNR) method we used to extract data with nickel layer from the low signal. We considered and excluded the possibility that other species might contribute to the lidar signal. The Ni layer is detected through absorption in the $3d8(3F)4s2 \rightarrow 3d9(2D)4p$ transition at 337.1 nm and re-emission in both the $3d9(2D)4p \rightarrow 3d8(3F)4s2$ and $3d9(2D)4p \rightarrow 3d9(2D)4s$ transitions at 337.1 and 339.4 nm respectively. Results from wintertime lidar observations on two nights (27-28 November 27-28 and 20-21 December 2012) at Chatanika, Alaska (65°N, 147°W) are presented. The wintertime Ni layer has a peak concentration of $1.0X10^4$ cm^-3 at 87 km with a column abundance of $1.8X10^{10}$ cm^-2, centroid height of 88 km and rms width of 6.6 km. The midwinter abundance of mesospheric iron (Fe) is $3.4X10^{10}$ cm^-2 indicating an Fe to Ni ratio of 1.9 in the upper atmosphere. This is significantly lower than the value of 18 for the ratio of Fe to Ni in chondrite meteorites. These observations are discussed in term of recent satellite observations of the Ni and Fe airglow.

MLTL-09   Midlatitude Mesospheric Temperature Anomalies During Major SSW Events as Observed with Rayleigh-Scatter Lidar - by Sox, Leda

Status of First Author: Student IN poster competition, PhD

Authors: Vincent B. Wickwar, Chad Fish, and Joshua P. Herron

Abstract: While the mesospheric temperature anomalies associated with Sudden Stratospheric Warmings (SSWs) have been observed extensively in the polar regions, observations of these anomalies at midlatitudes are sparse. The original Rayleigh-scatter lidar that operated at the Atmospheric Lidar Observatory (ALO; 41.7°N, 111.8°W) in the Center for Atmospheric and Space Sciences (CASS) on the campus of Utah State University (USU) collected a very dense set of temperature data for 11 years, from 1993 through 2004. The temperatures derived from these data extended over the mesosphere, from 45 to 90 km. This work focuses on the extensive Rayleigh lidar observations made during seven major SSW events that occurred between 1993 and 2004, and aims to compile a climatological study of the midlatitude mesospheric temperatures during these SSW events. In order to determine the characteristics of the midlatitude mesospheric temperatures during SSWs, comparisons were made between the temperature profile on an individual night during a SSW event and the climatological (11-year average) temperature profile for that night. An overall disturbance pattern was observed in the mesospheric temperatures during these SSWs. It included coolings in the upper mesosphere, comparable to those seen in the polar regions, and warmings in the lower mesosphere.

MLTL-10   Wide Dynamic Range Acquisition for Lidar - by Thomas, David Matthew

Status of First Author: Student IN poster competition, Undergraduate

Authors: Thomas, David; Smith, John; Chu, Xinzhao

Abstract: Lidar enables studies of the upper atmosphere through the collection of photons scattered by particles in the atmosphere. However, the usable range of data is limited not only by power and aperture, but also by the ability to derive a signal from a high gain detector which is linear to the input photon flux. The rate of detected photons depends on the altitude from which the light is scattered, leading to pulse pileup and saturation of the detector for altitudes which can include the lower stratosphere and low-frequency photon counting for altitudes extending above the metal layer, for the case of resonance-fluorescence lidar. We present our investigation of a novel system which includes all-digital processing of a conditioned photomultiplier signal to extend the linear dynamic range for a wider range of photon fluxes. Wider linear dynamic range of the data acquisition system will enable the utilization of photomultipliers to collect data from a wider range of altitudes, thereby helping to make the concept of a whole atmosphere lidar, capable of resolving waves and tides through the complete atmospheric column, feasible.

MLTL-11 Extremely Sensitive Rayleigh-Scatter Lidar at USU - by Wickwar, Vincent B.

Status of First Author: Non-student

Authors: Vincent B. Wickwar, Leda Sox, David L. Barton, Joshua P. Herron, Matthew T. Emerick

Abstract: We have and are developing an extremely sensitive, midlatitude, Rayleigh-scatter lidar at the Atmospheric Lidar Observatory (ALO), part of the Center for Atmospheric and Space Sciences (CASS), on the campus of Utah State University (USU). This is a major upgrade from the original Rayleigh-scatter lidar that operated from 1993 through 2004. The original lidar had a figure of merit, power-aperture product (PAP), of ~3.1 Wm2, whereas the new lidar has a PAP of 205 Wm2. This 65 times increase in sensitivity is achieved by a combination of increasing the collecting area from 0.15 m2 to almost 5 m2 and almost doubling the laser power to 42 W at 532 nm. The immediate effect is to increase the maximum altitude upward from 90 km. Initial temperatures with the new system have been obtained up to 115 km and we are aiming at regular temperature measurements up to 120 km. This puts us into new territory for ground-based observations. With additional detector channels, needed to accommodate the dynamic range and different types of atmospheric scattering processes, we will extend the observations downward to ~15 km. Below 35 km this will additionally involve Mie scatter from aerosols and Raman scatter from N2. The greater sensitivity will help with the Raman scatter, because its cross section is almost 1000 times smaller than the Rayleigh cross section. The overall scientific gain will come from the new ability to simultaneously observe most of the middle atmosphere from the lower stratosphere, through the mesosphere, into the lower thermosphere with a single ground-based instrument.

MLTL-12 Roles played by E-field, vertical wind and aurora in the source and formation of thermospheric Fe/Fe+ layers at high latitudes - by Yu, Zhibin

Status of First Author: Student NOT in poster competition, PhD

Authors: Zhibin Yu and Xinzhao Chu

Abstract: As the lower boundary of ionosphere and space weather regime, the mesosphere and thermosphere is a chemically and dynamically complex and important region. The roles of atmospheric gravity waves in transporting energy and momentum and causing atmospheric and ionospheric disturbances have been recognized by theoretical studies and observational evidence. The thermospheric neutral Fe layers discovered by the Chu lidar group at McMurdo (77.8S, 166.7E), Antarctica, exhibit well defined gravity wave signatures in the altitude range of 110~155 km. Those thermospheric Fe layers provide an excellent trace for measuring neutral temperature and winds in the thermosphere. Our theory argues that the observed Fe layers are a result of coupling of electrodynamical, neutral dynamical and chemical processes.

Stimulated by the understanding of the new observations, a time-dependent, 1-D, high-latitude Fe/Fe+ model has been developed to simulate the observed Fe profiles based on the first principles of physics and chemistry. In this paper, we will provide quantitative analyses of formation of thermospheric Fe atoms and confirm that they are produced by neutralization of converged Fe+. We will further quantitatively demonstrate that gravity wave wind shear creates Fe+ layers of enhanced density. The simulations of Fe layers are consistent with the observations. Besides the wind-shear mechanism, electric field cause upward flow transporting Fe+ ions from the main deposition region into the thermosphere. At the same time, electric field can help convergent but can also destroy wind-shear-converged Fe+ layer, depending on the relative phase. In this paper, the competitions between wind-shear and electric field driving forces will be investigated to study the neutral-ion (Fe/Fe+) coupling. In our simulations, the role of auroral electron precipitation on the formation of thermospheric Fe layers is quantified. Our observational data also show that gravity-wave-driven neutral Fe layers are modulated by longer period waves or tides. These events will also be examined by our numerical model.

MLTL-13   **Observation of Sporadic Sodium Layer at a low-latitude location, China by Lidar -** by Zhang, Tiemin

Status of First Author: Non-student

Authors: Tiemin Zhang, Fuheng Zhang, Dali Yang, Xianchang Yang, Jihong Wang, Jun Fu

Abstract: Na lidar observations of SSL at a low-latitude location (Haikou, China, 20 oN, 110 oE) during 2010 are reported in this paper. From 38 SSL events detected in about 458 h of observation, a SSL occurrence rate of 12.0 h at our location is obtained. The statistical analyses of main parameters for the 39 SSL events are made, and the results are compared with those of other location reported. By examining the corresponding data from about 160 km southwest ionosonde, it was found that there was some correlation between SSL and Es. Of the 20 pairs of SSL and Es events checked, 20 pairs of them were correlated within 1 h in time.

MLTL-14   **New scientific frontiers in resonance-fluorescence Doppler lidar –** by Smith, John A.

Status of First Author: Student IN poster competition, Masters

Authors: John Smith and Xinzhao Chu

Abstract: Resonance-fluorescence Doppler lidars have historically been plagued by depressed signal levels and low SNR. New approaches that we have developed for the design of resonance lidar receivers, both nighttime and daytime, has led to giant leaps in performance, opening up totally new avenues for scientific inquiry in the space-atmosphere interaction region (SAIR). Efficiency gains have been so significant that the modest 0.5 W/0.81 m power-aperture product lidar system on which these techniques were developed has matched the signal levels of the highest power-aperture resonance Doppler lidars ever operated- those operated during short-term campaigns at the 1.35 W/3.5 m Starfire Optical Range (SOR) and the 1.35 W/3.67 m Air Force Research Laboratory AEOS facility at Maui. With faster control and acquisition electronics developed since then, we have reduced the temporal integration period by a factor of 30, to 3 seconds per profile, enabling MLT temperature and wind retrieval with resolutions sufficient to resolve seasonal, full diurnal vertical eddy flux in the MLT region for the first time by lidar.

Mesosphere or Lower Thermosphere General Studies

MLTS-01 **Heating Efficiency from the Exothermic Reaction of H with O3 -**
by Smith, Anne

Status of First Author: Non-student

Authors: Anne K. Smith, Manuel Lopez-Puertas, Jiyao Xu, Martin G. Mlynczak

Abstract: Exothermic reactions provide much of the heating in the MLT region. The reaction of H and O3 is the dominant exothermic heating source around 80-95 km. Not all of the energy from this reaction is converted to heat; some is lost to airglow in the Meinel bands. Up to now, the WACCM chemistry climate model has used a specified efficiency of 0.6 (i.e., 60% of the energy of the reaction is converted to heat). Here, we use a model of the vibrationally excited OH produced by the reaction to determine the efficiency of heating. The model of the OH vibrational system is used interactively with the WACCM temperature and composition at each model gridpoint and timestep. In the global mean, the efficiency at the altitudes where the heating is largest varies with altitude between 0.6 and 0.65. Locally the range of values is wider. Both the heating rate and its efficiency increase where the atomic oxygen concentration increases; in the polar winter the efficiency can be greater than 0.75.

Mesosphere and Lower Thermosphere Other Tidal, Planetary Waves, or Sudden Stratosphere Warnings

MLTT-01 **Planetary Wave Variability of Sq Currents -** by Elhawary, Reham

Status of First Author: Student IN poster competition, PhD

Authors: J. M., Forbes and Q. Wu

Abstract: The E-region wind dynamo represents a key linkage in atmosphere-ionosphere coupling, due to its generation of electric fields that permeate the ionosphere. Measurement of ground magnetic variations due to dynamo-region currents is one means of gaining insight into variability of this process, yet very little is known about variability of the solar-quiet (Sq) current system in terms of its connections with atmosphere dynamics. In this work we quantify the variability of ground magnetic perturbations at the mid-latitude station of Stennis Space Center (BSL) (30.3507°N, 89.6359°W) during Sept 2008-Sept 2010, with specific focus on planetary wave variability. We find distinct signatures with periods close to those of well-know normal modes, i.e., 5-, 10-, and 16-days, and various features of these signatures are described. Comparisons are also made with co-located TIME/TIDI measurements of winds near 110 km, and similarities and differences with the magnetic variations are evaluated.

MLTT-02 **Effects of the El Nino-Southern Oscillation and the Quasi-Biennial Oscillation on the Diurnal tides -** by Barrett, Adam

Status of First Author: Student IN poster competition, Masters

Authors: Adam C. Barrett and Jian Du

Abstract: The eCMAM30 data (the extended Canadian Middle Atmosphere Model nudged to reanalysis data from 1979 to 2010) are used to study the effects of the Quasi-Biennial Oscillations (QBO) and the El Nino Southern Oscillations (ENSO) on the diurnal tides (wavenumber from -5 to 5). The effects of QBO and ENSO are difficult to disentangle, and will use the following the method outlined in Garfinkel and

Hartmann (2007) to isolate each effect from the other. Composite are taken of QBO months under near-neutral ENSO conditions to examine the effect of QBO on the diurnal tides. Because of the bimodality of QBO, producing a meaningful composite of ENSO months under near-neutral QBO is difficult, as the number of available months in quite small. To distinguish ENSO from QBO and to further study the QBO, we compare composites of months with four different combinations of QBO and ENSO anomalies (Warm-ENSO/West-QBO, Warm-ENSO/East-QBO, Cold-ENSO/East-QBO, and Cold-ENSO/West-QBO). The effects of ENSO and QBO on the diurnal tides will be investigated and tested for significance in this analysis.

MLTT-03   **Simulation of the 16-day wave in the stratosphere and mesosphere using TIME-GCM and MERRA -** by Nguyen, Vu Anh

Status of First Author: Student IN poster competition, PhD

Authors: Vu Nguyen, Loren Chang, Scott Palo, Han-Li Liu

Abstract: Past observations have shown that the effects of the quasi 16-day planetary wave, representing the second symmetric Rossby normal mode, are prevalent throughout the middle atmosphere and occasionally, some portions of the upper atmosphere. In the presented work, we investigate the mechanisms driving the propagation of the quasi 16-day planetary wave from a source in the lower atmosphere to higher altitudes by using the NCAR Thermosphere Ionosphere Mesosphere Electrodynamics General Circulation Model (TIME-GCM). The quasi 16-day planetary wave is simulated in the model by introducing perturbations in geopotential height at the lower boundary of the model and comparing it to a control run. Analysis of the model runs over the course of a year show that the background zonal wind is the main driver in inducing seasonal changes in the quasi 16-day planetary wave structure. Derived quasi-geostrophic potential vorticity gradient and Eliassen-Palm flux from the model output also shows that the penetration of the wave into regions of mean wind instability only plays a minor role in wave amplification. A comparison of the 16-day wave in the TIME-GCM to MERRA displays differences that can be attributed to contrasting background zonal mean winds. To achieve a more realistic simulation of the 16-day wave, the background zonal winds in the TIME-GCM are nudged to the background zonal winds in MERRA.

MLTT-04   **Tidal Variability Due to the Quasi-biennial Oscillation and Ionospheric Responses -** by Wang, Jack Chieh

Status of First Author: Student IN poster competition, Masters

Authors: Jack C. Wang, Loren C. Chang, Qian Wu, Charles C.H. Lin[1]
[1] Department of Earth Sciences, National Cheng Kung University, Tainan, Taiwan

Abstract: The Quasi-biennial Oscillation (QBO) is a persistent oscillation in the zonal mean zonal winds of the low latitude middle atmosphere that is driven by breaking planetary and gravity waves, with a period near two years. The atmospheric tides that dominate the dynamics of the mesosphere and lower thermosphere region (MLT, between heights of 70 to 120 km) are excited in the troposphere and stratosphere, and propagate through QBO-modulated zonal mean zonal wind fields. This allows the MLT tidal response to also be modulated by the QBO, with implications for ionospheric/thermospheric variability. In this research, we develop an empirical model to isolate QBO-related tidal variability in the MLT diurnal and semidiurnal tides using values from assimilated TIMED satellite data. Tidal fields corresponding to QBO eastward and westward phases are then used to drive the NCAR Thermosphere-Ionosphere-Electrodynamics General Circulation Model (TIE-GCM), and differences in major ionospheric / thermospheric features examined.

MLTT-05   Automated Computation of Hough Modes at Higher Wave-Numbers Using MATLAB - by Warder, David M.

Status of First Author: Student IN poster competition, Undergraduate

Authors: David M. Warder and Jian Du

Abstract: Hough mode wave decomposition is a method developed in 1898 by S.S. Hough to characterize a fluid wave as a series of fundamental waves that are latitude-dependent solutions to an eigenvalue-eigenfunction problem. Utilizing MATLAB, we can automate a significant portion of the Hough mode calculation process, enabling the calculation of a large number of wave numbers and periods and their associated latitude profiles. The process of calculation will be demonstrated and the resultant data subjected to brief analysis; the comparison of the results with the Extended Canadian Middle Atmospheric Model (ECMAM) will also be discussed.

Sprites

SPRT-01   Possible Sources of Ionospheric Inhomogeneities Initiating Sprite Streamers - by Liu, Ningyu

Status of First Author: Non-student

Authors: Ningyu Liu (nliu@fit.edu), Hans C. Stenbaek-Nielsen (hnielsen@gi.alaska.edu), and Matthew G. McHarg (Matthew.Mcharg@usafa.edu)

Abstract: Sprites are large, luminous electrical discharges above thunderstorms, which can span the 40-90 km altitude range. They are caused by intense cloud-to-ground lightning (CG) flashes that temporarily produce a strong quasi-electrostatic field in the upper atmosphere. The dominant filamentary structures observed in sprites are typically tens to hundreds of meter wide, and they are known as streamers [e.g., Pasko et al., GRL, 25, 2123, 1998; Liu and Pasko, JGR, 109, A04301, 2004].

Recent high-speed images indicate that sprite streamers are often initiated from luminous structures in the lower ionosphere [Stenbaek-Nielsen et al., Surv. Geophys., 34, 769, 2013, Qin et al., Nat. Comm., doi: 10.1038/ncomms4740, 2014]. Theoretically, it has been recently concluded that inhomogeneities are required for sprite streamer initiation [e.g., Qin et al., JGR, 116, A06305, 2011, Liu et al., PRL, 109, 025002, 2012, Kosar et al., JGR, 117, A08328, 2012, Kosar et al., GRL, 40, 6282, 2013]. However, it is unknown what processes in the lower ionosphere produce those inhomogeneities.

In this talk, we investigate the possible sources of the ionospheric inhomogeneities that lead to sprite streamer initiation when subject to the lightning field. We will show numerical simulation results and high-speed video observations on sprite streamer initiation.

SPRT-02   GPS Timing for Simple, Automatic Camera Systems to Observe Transient Luminous Events - by Morrison, Michael Dwayne

Status of First Author: Student IN poster competition, Undergraduate

Authors: Michael Morrison, Nicholas Spiva, and Ningyu Liu

Abstract: Transient luminous events (TLEs) have recorded lifetimes from a few milliseconds up to about one second [e.g., Pasko, J. Geophys. Res., 115, A00E3, 2010]. In order to accurately measure the time evolution of an event, the time recording device should have millisecond precision. Many simple camera

systems use a GPS time stamping device to faithfully insert the correct time on the video images. A typical system also contains a backup timing mechanism to double check the GPS time stamped on the images.

The TLE camera system at Florida Institute of Technology uses a WATEC 120+ low light camera connected to a KIWI OSD video time inserter for time stamping the video. The WATEC 120+ camera is set up to capture 60 video fields per second and passes the fields to KIWI. The KIWI OSD is a GPS time clock with an internal quartz crystal to control the field rate counter. In this talk, we investigate the accuracy of the GPS time given by a video time inserter like KIWI OSD.

In addition, we are currently constructing a new digital TLE camera system using an ASI120MM camera. Switching to digital images will provide sharper images and a faster frame rate around 100 frames per second; however, at this time, there is no accurate method of time stamping a USB signal. Here, we discuss potential solutions to this problem and present our testing results.

SPRT-03   Estimation of Locations and Altitudes of Upward Electrical Discharges Observed Above Tropical Depression Dorian - by Spiva, Nicholas

Status of First Author: Student IN poster competition, Undergraduate

Authors: Nicholas Spiva, Michael Morrison, Ningyu Liu

Abstract: Jets and Gigantic Jets are electrical discharges that form inside the cloud, escape the cloud top and propagate upward. Gigantic jets create an electrical connection between the cloud top, in the upper part of the troposphere, at about 15-20 km, and the lower ionosphere, at about 80-90 km [Pasko et al., Nature, 416, 152, 2002; Krehbiel et al., Nat. Geosci., 1, 233, 2008]. The existence of these phenomena is a relatively new discovery [e.g., Wescott et al., Geophys. Res. Lett., 22, 1209-1212, 1995], so there has been a lot of research work being done to understand those phenomena in our atmosphere.

On 2 August 2013, the Geospace Physics Lab at Florida Tech captured videos of six jet events and one blue starter event above Tropical Depression Dorian. Of the six jet events, four of them are classified as 'gigantic jets' and two as regular jets. In order to analyze the development of these events, their accurate locations and altitudes must be determined. In this talk, we present an analysis combining star-fields with the data from National Lightning Detection Network (NLDN) to determine those important parameters.

To conduct the analysis, we first enhanced the contrast of the original images to make stars clearly visible. Once a handful of stars were visible, they were identified by using Stellarium. We then used the Graphical Astronomy and Image Analysis tool (GAIA), which fits the stars in the image to a star map and gives the Right Ascension / Declination for each pixel in the image. The RA/Dec coordinates were then converted to azimuth and altitude angles, which gave the direction from the camera at Florida Tech to each pixel, as well as the apparent altitude of the base from the horizon. The recorded lightning strokes from the NLDN were then plotted on a weather map with the infrared radar image of the storm overlaid. The azimuthal angles of the events were then plotted on the map as well. Finally, the locations of the events were estimated based on the lightning strokes around the respective azimuthal directions, taking into account the proximity in time from the lightning events to the jet events. Once the locations were determined, altitude measurements could then be made on the events, allowing for the size and speed of the events to be calculated.

Agner, Ryan Matthew, 14
Aguilar Guerrero, Jaime, 15

Barjatya, Aroh, 5
Barrett, Adam, 28
Barry, Ian Forest, 21
Barton, David Lee, 22

Cai, Xuguang, 22
Cao, Bing, 15
Carstens, Justin Neal, 15
Cook, Matthew W, 4
Cullens, Chihoko Yamashita, 16

Dawkins, Erin, 9
DiMenichi, Chris, 8
Drob, Douglas Patrick, 3

Elhawary, Reham, 28
Evans, Wayne F.J., 14

Fisher, Daniel J, 16
Fletcher, Alexander, 10
Fong, Weichun, 23

Gan, Quan, 8
Gao, Boyi, 10
Gao, Qi, 23
Gasperini, Federico, 1
George, Richard, 17
Gerding, Michael, 24
Grawe, Matthew A, 1
Gu, Sheng-Yang, 1
Guo, Yafang, 17

Haeusler, Kathrin, 3
Hall, Stephen, 18
Heale, Christopher, 18
Huang, Wentao, 24

Jones, Jr., McArthur, 2

Kim, Jeong Han, 2
Kristoffersen, Samuel, 7

Li, Jintai, 25

Limonta, Lorenzo, 11
Lin, Charles, 4
Liu, Ningyu, 30
Lu, Xian, 18, 19

Mehta, Dhvanit, 19
Michael Dwayne, 30

Negale, Michael R, 16
Nguyen, Vu Anh, 29
Nielsen, Kim, 19
Nischal, Nirmal, 9

Pugmire, Jonathan, 20

Rainville, Nicholas, 5
Robinson, Rebecca Anne, 6

Salem, Mohammad A, 3
Scipion, Danny Eddy, 6
Smith, Anne, 28
Smith, John A, 27
Sox, Leda, 25
Spiva, Nicholas, 31
Stark, Johnathon, 7
Sugar, Glenn, 11

Tarano, Ana Maria, 12
Thomas, David Matthew, 25
Triplett, Colin Charles, 9

Vail, Christopher, 20
Vargas, Fabio, 21
Volz, Ryan, 12

Wang, Jack Chieh, 29
Warder, David M, 30
Westerhoff, John, 7
Wickwar, Vincent B., 26

Yang, I-Ching, 12
Yee, Jonathan, 13
Yu, Zhibin, 26

Zhang, Tiemin, 27
Zhu, Qian, 13